P6.16 **DAYTIME BOUNDARY LAYER HEIGHTS OVER THE ALPS. AN OBSERVATIONAL AND NUMERICAL STUDY**

Stephan F.J. De Wekker[1]*, D.G. Steyn[1], S. Nyeki[2]

[1] Atmospheric Science Program, The University of British Columbia, Vancouver, BC, Canada
[2] The University of Essex, Colchester, England

1. INTRODUCTION

Mountain ranges can strongly modify the height of the daytime convective boundary layer (CBL). Observations show a variety of behaviours, ranging from CBLs that follow underlying terrain to CBLs that seem unaffected by terrain (De Wekker et al. 1997; Kalthoff et al. 1998; Koßmann et al. 1998). CBL heights in these studies were determined primarily from vertical temperature profiles. In recent years, the development of remote sensors has provided alternatives for the determination of CBL heights. Particularly downward looking airborne lidars (light detection and ranging) have proven to be very useful for the investigation of spatial variability of CBL heights (e.g., Melfi et al. 1985; Kiemle et al. 1995).

During the STAAARTE '97 field study, a downlooking lidar was carried aboard an aircraft that flew over the European Alps to investigate the spatial variability of the CBL height over mountainous terrain. Preliminary results from this field study were presented by Nyeki et al. (2000). Based on the lidar observations, it was concluded that CBL heights did not follow topography. Unfortunately, no observations of the thermodynamic structure of the atmosphere were available in the region of interest to confirm this conclusion.

In the present paper, the observed behaviour during STAAARTE '97 is investigated in more detail with a numerical mesoscale model. This approach of combining observed phenomena with output from mesoscale model simulations has previously proven useful for investigating the spatial variability of CBL heights over mountainous terrain (De Wekker et al. 1998). In the present paper, CBL heights are determined from model output and compared with lidar observations. Based on model results, a new interpretation of the lidar data is given, providing a more complete picture than can be determined by observations alone. In addition, lidar and mesoscale model data are compared with CBL heights from the ECMWF model for a grid cell in the area of interest. ECMWF provides these CBL heights on an operational basis for use as input to air pollution models.

2. DATA

Under the European Union's "Scientific Training and Access to Aircraft for Atmospheric Research Throughout Europe" (STAAARTE) project, an airborne campaign was conducted in an area of approximately 0.5ºx0.5º around the Jungfraujoch high-alpine research station (JFJ, 46.55º N, 7.98º E; 3580 m) on 30 July 1997. A nadir-pointing aerosol lidar aboard the German Aerospace Research Establishment (DLR) Falcon 20 jet aircraft (Kiemle et al. 1995) obtained a data set with high temporal and spatial resolution of the aerosol structure below 5 km.

The JFJ belongs to the northern slope of the Swiss Alps and is situated in a saddle between the Mönch (4099 m) and Jungfrau (4158 m). South of the JFJ the Aletsch glacier dominates the topography. Topography around the JFJ is shown in Fig. 1b.

Lidar measurements consisted of a morning and afternoon flight pattern over the JFJ. Flight patterns consisted of transects within a 0.5ºx0.5º domain, oriented parallel and perpendicular to the regional mountain divide (NE-SW). A total of 35 flight legs were flown. 17 legs took place in the morning between 0628 and 0925 UTC, and 18 legs between 1247 and 1533 UTC, each

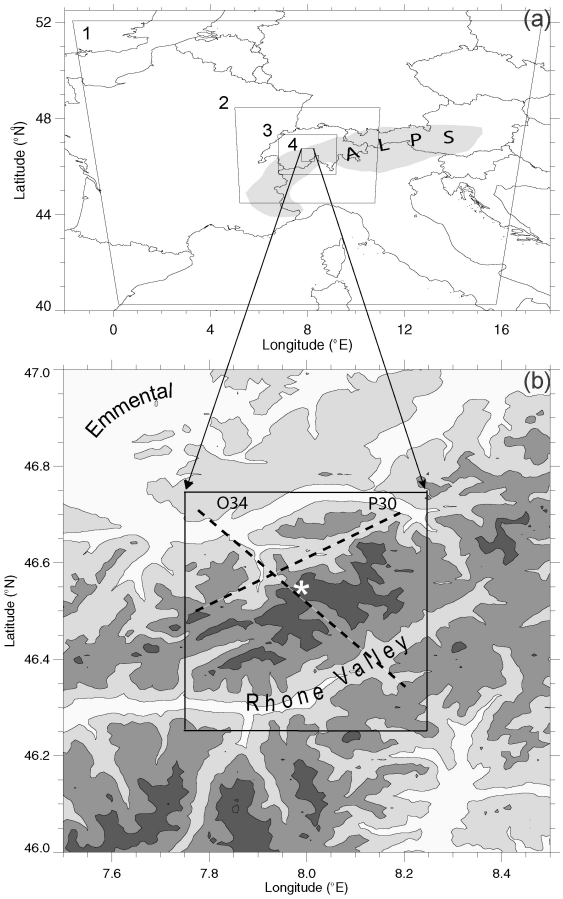

FIG. 1. Map of Europe with the four grids in RAMS represented by the rectangles (a). The innermost grid is shown in detail in (b). Contour lines are drawn every 1000 m, the darkest shade represents terrain over 3000 m asl. The Jungfraujoch station is depicted by the white asterisk. Two flight tracks, O34 and P30, are depicted by the dashed lines.

**Corresponding author address*: Stephan F.J. de Wekker, Atmospheric Science Program, Department of Earth and Ocean Sciences. The University of British Columbia, Vancouver, BC, V6T 1Z4, Canada, e-mail: sdewekker@eos.ubc.ca

leg lasting between 2 and 8 minutes. The vertical and horizontal resolution of the dataset was 15 m and approximately 100 m, respectively. The NW-SE transect represents the sharp transition in topography from the pre-alpine foothills in the Emmental region (up to ~2000 m), through the JFJ and surrounding massif (3000-4000 m) and down over the Aletsch glacier towards the Rhone valley. The dashed lines in Fig. 1b depict flight tracks in the area (discussed in section 4). Pre-alpine land use consists largely of urban, agricultural and forested areas, changing to snow and glaciated cover above the snowline at 2500 m in late summer.

The weather situation on 30 July 1997 was characterized by cloudless skies over large parts of Europe with a high pressure ridge from Scandinavia to France. Synoptic winds at 700 mb were weak to moderate and from northwesterly directions. In the afternoon, convective clouds developed occasionally over the Alps.

3. MODEL

The numerical mesoscale model used is the Regional Atmospheric Modeling System (RAMS). RAMS (Pielke et al. 1992) is a non-hydrostatic model with a terrain-following coordinate system employing a Mellor-Yamada level 2.5 turbulence closure scheme. RAMS employs a surface parameterization scheme in which surface turbulent fluxes are calculated according to the Louis (1979) parameterization. Land-surface processes are represented by the Land Ecosystem Atmosphere Feedback Model, version 2 (Walko et al. 2000). The presence of snow covered surfaces and glaciers is also accounted for in this model. The 3-D simulations use two-way interactive, nested grids. The model domain consists of four nested grids with horizontal grid spacing of 27, 9, 3, and 1 km, respectively. The four grids are depicted in Fig. 1a. The outermost grid covers central Europe including the Alps while the innermost grid is shown in more detail in Fig. 1b. All four grids have 53 vertical levels, with a grid spacing from 50 m near the surface, to 160 m at 2000 m agl to 1000 m near the model top at about 16 km. Terrain height and land use were obtained from standard USGS datafiles. The simulations cover 36 hours, from 1200 UTC 29 July to 0000 UTC 30 July 1997. The five outermost lateral boundary points in the largest domain were nudged toward NCEP objective analysis fields and rawinsonde data to allow changes in large-scale conditions to influence the model simulations. The model output was evaluated with temperature- and wind data from aircraft and selected surface and rawinsonde stations around the investigation area. The correspondence between observations and model output was good.

4. RESULTS

4.1 Observations of the aerosol layer height

Figure 2a and 2b show lidar cross sections along flight tracks P30 and O34, respectively. The location of these tracks is depicted in Fig. 1b. Flight track P30 was heading northeast from 1409 to 1413 UTC while O34 was heading southeast from 1520 to 1525 UTC. The shading on the cross sections represents backscatter intensities, with dark shading showing clean air and light shading representing aerosol-laden air. The topography is indicated in white. The white vertical lines are caused by the presence of clouds. The height of the aerosol layer (AL) can be visually detected by the transition between high and low backscatter intensities. For an objective determination of the AL height, several sophisticated schemes were attempted. Because these methods did not work well for many backscatter profiles encountered in the dataset, we reverted to the simple method of defining a region in the lower part and in the upper part of the atmosphere where the backscatter ratios are fairly uniform. The average value of the backscatter values found in these two regions was taken as the threshold value. The location where this value was first exceeded starting from the top of the profile was defined as the AL height. After the method was applied to the data, further analysis included visual scanning of the AL heights to detect any failures of the algorithm. These failures occurred, e.g., at locations where convective clouds were present. The resulting values are shown by the white dots in Fig. 2a and 2b. It can be seen clearly that the AL height seems rather unaffected by the small-scale topography, with values around 4 km asl. Figure 2a shows that there is a tendency for the AL height to follow the large-scale topography somewhat, with decreasing aerosol heights towards the northwest. The two examples shown here are representative of the other lidar cross sections on the afternoon of this case study.

4.2 CBL heights from model output

CBL heights were determined from RAMS output with a Richardson number (*Ri*) approach following Vogelezang and Holtslag (1996). *Ri* is calculated at each model level starting from the surface and the CBL height is derived by linear interpolation between the level where *Ri* becomes larger than 0.25, and the level below. For sake of comparison, the parcel method was also applied. In this method, CBL height is determined as the equilibrium level of a hypothetical rising parcel of air representing a thermal. For this method, lower heights were found ($0.9<r<1$) than for the *Ri*-method, because shear generated turbulence is neglected.

Figure 2c and 2d show cross sections of modeled potential temperature from RAMS. Dashed lines indicate the CBL height calculated with the above procedure. The locations of the cross sections are similar to Figs. 2a and 2b. Differences in the topography are partly due to a flight track that was not entirely straight. Figure 2d shows that CBL heights were higher south of the JFJ where the average terrain elevation is higher. In general, it can be seen that the CBL height follows the terrain to some extent but also that the large static stability in the upper layers inhibits the CBL from becoming very deep. The stable layer was also found in radiosonde profiles at stations around the area, which provides support for the CBL heights determined from RAMS.

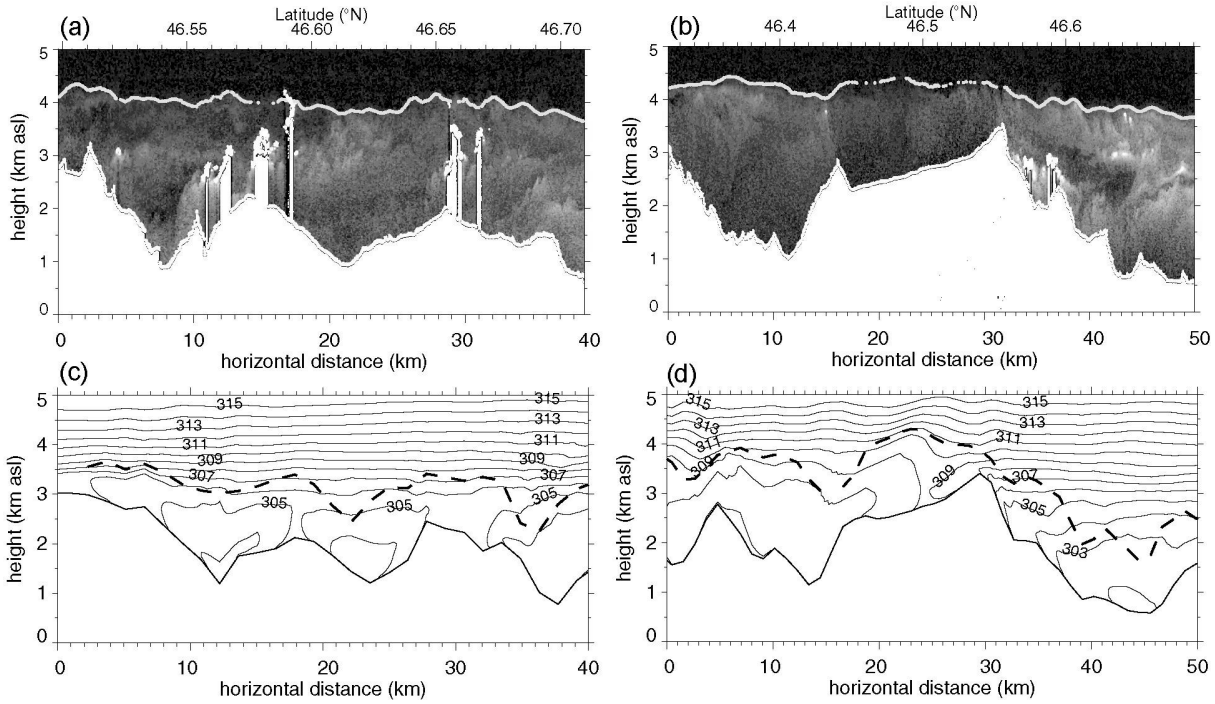

FIG. 2. Cross sections of backscatter intensity for flight tracks P30 (a) and O34 (b). The gray scale is proportional to lidar backscatter with light colors indicating high backscatter intensities. The aerosol layer height is depicted with the white dots. (c) and (d) are cross sections of modeled potential temperature (in K) for the same track as in (a) and (b), for 1400 and 1500 UTC, respectively. CBL height is depicted by a dashed line.

5. DISCUSSION

Observed AL heights and CBL heights from RAMS were compared for all flight tracks in a fashion similar to Fig. 2. The comparison indicates that CBL heights show a larger spatial variability and are generally lower than AL heights. Differences can be very significant, from a few hundred meters up to one kilometer. Only south of the JFJ, where terrain elevations are highest, there is a better correspondence between both heights.

Previous studies over flat terrain have also found consistently larger AL height from lidar data, compared to CBL heights from temperature profiles (e.g., Coulter, 1979). Differences in those studies are not as large as in the current study, though. The discrepancy in the studies over flat terrain is explained by the fact that the most energetic thermals can penetrate through the stable layer and carry aerosols above the CBL height. This process can be even more important over mountainous terrain. It is well known that thermals can be more vigorous over mountain slopes and ridges (e.g., WMO, 1993). When thermals reach lifting condensation level, clouds can become an efficient agent to detrain polluted boundary layer air into more stable layers aloft (Ching et al. 1988). This becomes an even more efficient process once the clouds reach their level of free convection. In many of the 35 lidar cross sections in the present study, there was evidence for the existence of clouds, suggesting that cloud venting may be one of the possible mechanisms that caused the AL height to be higher than the CBL height. Another mechanism that can become important over mountainous terrain is advective venting if the horizontal windvector crosses the inhomogenous CBL top (Koßmann et al. 1999). The advection of aerosols from different airmasses upwind of the area of interest can also be an important process for the existence of aerosols in layers above the CBL height. The picture that emerges from the comparison of the observational and modeling results along with the possible mechanisms that explains the observed aerosol structure, is summarized in Fig. 3. Unfortunately, the origin of the aerosols cannot be determined from the observations or model output so that the contribution of the various mechanisms cannot be investigated further.

A comparison of observed aerosol heights with CBL heights from RAMS output and ECMWF output is presented in Fig. 4. AL heights were determined semi-objectively in the way described in section 4.1 for 7 out of the 17 morning flight tracks and 12 out of the 18 afternoon flight tracks. The other flight tracks were not well-suited for determination of AL heights. The black circles in Fig. 4 represent averages of all the observed heights in one flight track (for sake of comparison with ECMWF data). CBL heights were determined from RAMS output following Vogelezang and Holtslag (1996, see section 4.2) for each hour from 0800 to 1700 UTC. The squares in Fig. 4 represent averages over all the gridpoints in the innermost grid. It thus represents an average for a 0.5° x0.5° area. The diamonds represent CBL heights determined from ECMWF output, also determined according to the Vogelezang and Holtslag method. The value is for an ECMWF gridpoint located at 46.5ºN, 8ºE (ECMWF model resolution is 0.5° x0.5°). It is seen that ECMWF CBL heights correspond more with

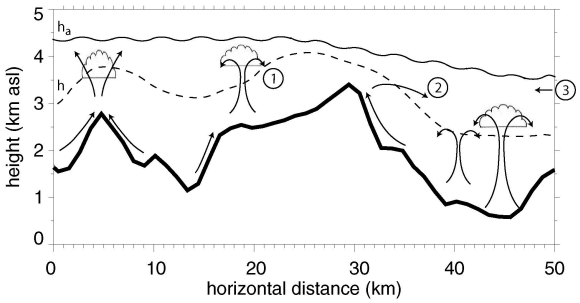

FIG. 3. Conceptual picture of the situation on the afternoon of 30 July 1997. h is the CBL height and h_a the AL height. The depicted processes are (1) cloud venting, (2) advective venting, and (3) advection of aerosols from airmasses elsewhere.

observed AL heights than RAMS CBL heights. Since the terrain elevation at the ECMWF gridpoint is lower than the average terrain elevation in the 0.5ºx0.5º grid box around it, differences in CBL depths (defined as the the difference between CBL height and terrain elevation) are even larger. Also, the differences in AL and RAMS CBL height seem to become larger during the afternoon. The question arises whether the CBL height or the AL height is the relevant 'mixing height' which is an important parameter in air pollution studies. This mixing height is defined as "*the height of the layer adjacent to the ground over which pollutants … become vertically dispersed by convection or mechanical turbulence within a time scale of about an hour*" (Beyrich et al. 1996). If mountain induced venting processes as illustrated in Fig. 3 play an important role in the mixing of pollutants, the mixing height defined in this way may be too small. For mountainous terrain, therefore, the definition would be more useful if it included the effects of these processes and their appropriate timescales. For time scales larger than a few hours, the current study indicates that AL heights may be a more appropriate length scale for air pollution considerations than CBL heights.

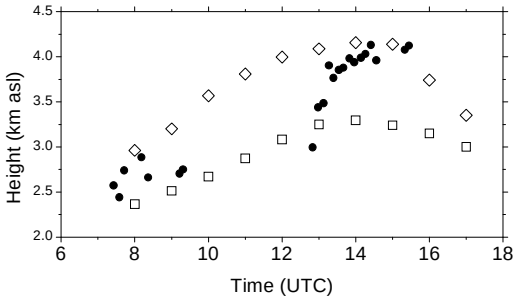

FIG. 4. Development of the AL from flight tracks (filled circles) and development of the CBL in a 0.5º x 0.5º area around the JFJ from RAMS (squares) and ECMWF (diamonds).

6. SUMMARY

Observations and model results indicate that AL heights were generally much larger than CBL heights during STAAARTE'97. Significant aerosol concentrations are often found above the CBL heights. It would be dangerous to generalize this conclusion based on one case study and further research is certainly required in this area. Mechanisms were suggested that cause aerosols to be transported to regions above the CBL height in mountainous terrain. CBL heights from the ECMWF model are much larger than CBL heights determined from a high resolution mesoscale model but are comparable with AL heights for this particular case study. The definition of mixing heights and the question whether the AL or CBL heights are the appropriate mixing height for air pollution studies in mountainous terrain was briefly addressed and needs more research. This study presents a case in which lidar observations alone could not provide conclusive information of the behaviour of the CBL height over the Alps. A numerical mesoscale model provided a useful tool for the investigation of the horizontally inhomogeneous boundary layer over mountainous terrain.

acknowledgments: We would like to thank Anton Beljaars for providing ECMWF boundary layer height data and Mathias Müller for his assistance in processing the lidar data. SdW was supported by a pre-doctoral Killam fellowship from the University of British Columbia. The research was partly funded by grants from NSERC. DLR and the EU Commission are thanked for their assistance and funding of the STAAARTE campaign.

REFERENCES

Beyrich F., et al., 1996: On the determination of mixing height: A review. Preprints 4th Workshop on Harmonization within Atmos. Disp. Mod. for Regulatory Purposes, 155-162.

Ching, J., et al., 1988: Evidence for cloud venting of mixed layer ozone and aerosols. *Atmos. Environ*., **22**, 225-242.

Coulter, R.L., 1979: A comparison of three methods for measuring mixing-layer height. *J. Appl. Meteor*., **8**, 1495-1499.

De Wekker, S.F.J., et al., 1997: Observations of daytime mixed layer heights over mountainous terrain during the TRACT field campaign. 12th Symp. on Bound. Layer & T., 498-499.

De Wekker, S.F.J., et al., 1998: Depressed mixed layer depths near a mountain base. 8th Conf on Mount Met., 373-379.

Kalthoff, N., et al., 1998: Temporal evolution and spatial variation of the boundary layer over complex terrain. *Atmos. Environ*., **32**, 1179-1194.

Kiemle, C., et al., 1995: The convective boundary layer structure from lidar and radiosonde measurements during the EFEDA'91 campaign. *J. Atm. Ocean. Technol*., **12**, 771-782.

Koßmann, M., et al., 1998: Aspects of the convective boundary layer structure over complex terrain. *Atmos. Environ*., **32**, 1323-1348

Koßmann, M., et al., 1999: Observations of handover processes between the atmospheric boundary layer and the free troposphere over mountainous terrain, *Contr. Atmos. Phys*., **72**, 329-350.

Louis, J.F., 1979: A parametric model of vertical eddy fluxes in the atmosphere. *Bound.-Layer Meteor*., **17**, 187-202.

Melfi, S. H., et al. 1985: Lidar observation of vertically organized convection in the planetary boundary layer over the ocean. *J. Clim. Appl. Meteorol*., **24**, 806-821.

Nyeki, S., et al., 2000: Convective boundary layer evolution to 4 km asl over high-alpine terrain: airborne lidar observations in the Alps. *Geophys. Res. Lett*., **27**, 689-692.

Pielke, R.A., et al., 1992: A comprehensive meteorological modeling system - RAMS. *Meteor. Atmos. Phys*.., **49**, 69-91.

Vogelezang, D.H.P., and A.A.M. Holtslag, 1996: Evaluation and model impacts of alternative boundary-layer height formulations. *Bound.-Layer Meteor*., **81**, 245-269.

Walko, R.L., et al., 2000: Coupled atmosphere–biophysics–hydrology models for environmental modeling, *J. Appl. Meteor*., **34**, 931–944.

WMO, 1993: Handbook of Meteorological Forecasting for Soaring Flights. WMO Techn. Note Nr. 495. 2nd edition.